BIOCELL
2021 45(4): 985-994

Tech Science Press

Fibroblast growth factor 9 promotes kidney cell proliferation via WNT signaling-mediated activation of *ANXA4*

Ting LI[1,#]; Xinhui SUN[2,#]; Nannan LI[1]; Hongmin GUO[2,*]

[1] School of Bioengineering, Wuhu Institute of Technology, Wuhu, 241003, China
[2] Department of Reproductive Medicine, Liaocheng People's Hospital, Liaocheng, 252000, China

Key words: Fibroblast growth factor, Kidney cell, Proliferation, ANXA4, WNT

Abstract: Fibroblast growth factors (FGFs) play pivotal roles in cell migration and proliferation. However, the identity of the FGF that plays a dominant role in kidney cell proliferation remains unclear. Therefore, in this study, we investigated the dominant FGF among all FGFs. To this end, RNA-sequencing, qRT-PCR, western blotting, and ChIP assays were performed. *FGF9* showed the highest expression among all FGFs, and its overexpression significantly promoted proliferation in the mouse kidney cell line C57BL/6 and increased JNK and AKT phosphorylation levels. Further, RNA-seq analysis identified 365 upregulated and 276 downregulated genes in *FGF9*-overexpressed cells. These differentially expressed genes were classified primarily into 20 biological pathways and were enriched in 31 gene ontology terms. qRT-PCR revealed that the expression of WNT and NF-κB signaling genes, as well as *ANXA4* expression patterns, correlated with the RNA-seq data, while *FGF9*-overexpressed cells accumulated more β-catenin, a key WNT signaling protein, compared to control cells. Moreover, downregulation of the gene that encodes *β-catenin* or *ANXA4* inhibited C57BL/6 cell proliferation. Additionally, the expression of *ANXA4* was lower in *CTNNB1*-knockdown cells than in the control group. Additionally, the ChIP assay revealed that a transcription factor complex containing TCF4 and β-catenin directly binds to the *ANXA4* promoter. Taken together, these results suggest a role of FGF9 in the regulation of kidney cell migration. These findings may prove useful in the development of future therapies.

Introduction

The kidneys are very important organs both morphologically and functionally as they serve to maintain salt, water, and acid-base homeostasis, as well as to secrete waste products in the form of urine (Márquez *et al.*, 2002). However, the intricate structure of the nephron is required for the kidney to carry out its function. Hence, kidney growth and maturation require the completion of nephrogenesis and further terminal differentiation (Nigam Sk and Brenner, 1996). Moreover, cell proliferation is a key process in organ development, and although previous studies have focused on morphological analysis during kidney development and the role of cell proliferation in nephron diseases (Márquez *et al.*, 2002; Song and Yosypiv, 2012; Lee *et al.*, 2015), reports detailing the underlying mechanisms associated with kidney cell proliferation, remain limited. Nevertheless, the studies that have been performed in this field have reported that hepatic nuclear factor-alpha (HNFα) regulates 14 downstream genes associated with kidney cell proliferation (Grigo *et al.*, 2008). Furthermore, although upregulation of fibroblast growth factor (FGF)9 and FGF1 was detected in adult rat kidney cortical and outer medullary tissues (Cancilla *et al.*, 2001), the function of these proteins in kidney cell proliferation during development is unclear.

The FGF family of proteins comprises 23 members in mammalian genomes (Mohammadi *et al.*, 2005); these are involved in regulating mammalian metabolism and development. Specifically, the role of FGFs has been characterized in embryogenesis, somitogenesis, body plan formation, gastrulation, skin wound healing, and organogenesis (Feldman *et al.*, 1995; Goldfarb, 1996; Martin, 1998; Sun *et al.*, 1999; Dubrulle and Pourquié, 2004; Kanazawa *et al.*, 2010). FGF1, specifically, has been shown to participate in blood sugar homeostasis via regulating insulin sensitivity (Suh *et al.*, 2014). Meanwhile, bFGF/FGF2 promotes skin fibroblast migration by activation of the PI3K-RAC1-JNK signaling pathway (Kanazawa *et al.*, 2010). Additionally, FGF21 has been reported to be highly sensitive to starvation stress or drug administration while also playing

*Address correspondence to: Hongmin Guo, guoguo8494@163.com
#These authors contributed equally to this work
Received: 28 June 2020; Accepted: 23 December 2020

Doi: 10.32604/biocell.2021.012371

a key role in glucose homeostasis, as well as in the protection of the liver and heart from injury (Lin *et al.*, 2013; Liang *et al.*, 2014; Lin *et al.*, 2014). In addition, FGF9 protects against fibrosis during cardiac fibroblast malformation (Sun *et al.*, 2019); meanwhile, abnormal activation of FGF9 during the development of the anorectum in rat embryos results in anorectal (Liu *et al.*, 2019). Still further, FGF23-klotho protects against early chronic kidney disease in Type 2 diabetes (Ribeiro *et al.*, 2019). However, the function of FGFs in kidney cell proliferation remains unclear.

A previous study using RNA-seq based transcriptome dissection reported that diverse pathway genes are under the control of bFGF, including WNT, hedgehog, and inflammatory response signaling genes in skin fibroblasts (Xuan *et al.*, 2016). Consequently, WNT/β-catenin signaling plays a key role in fibroblast migration and proliferation (Wang *et al.*, 2017). Additionally, the canonical WNT pathway, β-catenin-TCF/LEF-1 signaling, is reportedly activated by hepatocyte growth factor/scatter factor (HGF/SF), epidermal growth factor (EGF), insulin-like growth factor (IGF)-1, insulin, and IGF-2 (Muller *et al.*, 2002; Lu *et al.*, 2003; Deval *et al.*, 2006; Heo *et al.*, 2012). Furthermore, PI3K-activates PKB/AKT to phosphorylate GSK-3β at the Ser9 residue, thereby inhibiting GSK-3β activity and subsequently activating the β-catenin-TCF/LEF-1 axis in insulin signaling (Cross *et al.*, 1995; Weston and Davis, 2001). EGF stimulation also triggers the translocation of β-catenin to the nucleus to promote its transactivation irrespective of the stability and phosphorylation of β-catenin (by GSK-3β) (Lu *et al.*, 2003). In addition, EGF-ERK2 increases β-catenin transactivation and enhances α-catenin phosphorylation at Ser641 by CK2 to promote tumor cell invasion (Ji *et al.*, 2009). Meanwhile, β-catenin has been reported to promote cell proliferation in renal cancer cells (Yang *et al.*, 2017). Furthermore, a whole-genome aimed at identifying the sequences bound by the β-catenin-TCF/LEF transcription factor complex revealed that the TCF/LEF transcription regulation complex binds to the *cis*-element sequences $^{T}/_{A}{}^{C}/_{G}$AAAG present at downstream target gene promoters (Schuijers *et al.*, 2014). These findings indicate that diverse mechanisms modulate β-catenin activity (Lu and Hunter, 2004).

In the present study, the dominantly expressed FGFs were analyzed in kidney cells, and their associated regulatory mechanisms were characterized using molecular and biochemical assays. Consequently, this study identified the role of FGF9 in kidney cell proliferation and provided useful information for further exploration of the FGF-regulated cell proliferation mechanism.

Materials and Methods

Mouse kidney cell line culture

The C57BL/6 mouse kidney cell line was obtained from American Type Cell Collection (ATCC, Manassas, VA) and was grown in Dulbecco's Modified Eagle's medium (DMEM) containing 5.5 mM glucose, 1% penicillin-streptomycin, and 10% fetal bovine serum.

Cell proliferation analysis

Cell proliferation was measured using the Cell Counting Kit-8 (CCK-8, Dojindo Bio., Japan) following the manufacturer's instruction. Briefly, the cells (2.6×10^4 cells/well, 100 mL) were digested with trypsin and subsequently transferred to 96-well plates, with five parallel wells assigned for each treatment.

Overexpression of FGF9 and silencing of CTNNB1 and ANXA4 in C57BL/6 mouse kidney cells

The *FGF9* open reading frame was amplified from the cDNA of C57BL/6 mouse kidney cells by PCR and cloned into the pcDNA3.1 (+) (Cat. No. V79020; Thermo Fisher Scientific, Inc., Waltham, USA) expression vector to create *FGF9* overexpression plasmids. The primer information for *CTNNB1* silencing is shown as follow: FGF9 CF: ATGGCTCCCTTAGG TGAAGTTGG, FGF9 CR: TCAACTTTGGCTTAG AATATCCTTATA. The negative control siRNA (ON-TARGETplus si CONTROL non-targeting pool, D-001810) and *CTNNB1* siRNA duplex (ON-TARGET plus SMART pool, L-004018) were obtained from Dharmacon RNA Technologies (Chicago, IL, USA). RNAs (shRNAs) targeting *ANXA4* (shANXA4F: CGCGTccccCCGATGAAGACGCCATTATttcaa-gagaATAATGGCGTCTTCATCGGttttGGAAAT; shANXA4R: cgatTTCCaaaaaCCGA TGAAGACGCCATTATtctcttgaaAT-AATGGCGTCTTCATCGGGGGGA) and negative control non-specific shRNA (NC shRNA) were synthesized by Songon Biotech Co. (Shanghai, China; Liu *et al.*, 2017). Fibroblasts that reached 30%–50% confluence were used for transfection with 2 μg of the *FGF9* overexpression plasmid or 30 nM of the siRNA duplex using Lipofectamine 2000 (Invitrogen) and Opti-MEM® I Reduced Serum Medium (Gibco), according to the manufacturer's instructions.

RNA-sequencing assay

Total RNA extracted from C57BL/6 mouse kidney cells, with or without *FGF9*-overexpression, was used for RNA-sequencing experiments. The RNA-seq experiments and further data analyses were performed by Songon Biotech Co., Ltd. (Shanghai, China), and data were deposited in a personal computer, which will be released upon request.

GO and KEGG enrichment analyses

Differentially expressed genes were analyzed further based on statistical outcomes by assessing their association with biological processes using the gene ontology (GO) database (Consortium, 2006). Fisher's exact test was performed to enrich the GO category. The false discovery rate (FDR) was further calculated to correct the *P*-value, with a smaller FDR indicating a smaller error in judging the *P*-value (Dupuy *et al.*, 2007). The enrichment of GO terms among differentially expressed probe sets was identified using the one-tailed Fisher's exact test (Dunnick *et al.*, 2012). KEGG, Biocarta, and Reactome were employed to analyze pathway enrichment for differentially expressed genes. Fisher's exact test was followed by Benjamini–Hochberg (BH) multiple testing correction to select the significant pathways, and the threshold of significance was defined by *P*-value and FDR (Draghici *et al.*, 2007).

ChIP assay

Chromatin immunoprecipitation (ChIP) assay was performed using a chromatin immunoprecipitation assay kit (Cat No. 17-295, Millipore, Billerica, MA), according to the manufacturer's

instructions. Approximately 1 μg of anti-β-catenin antibody (Abcam, ab32572) or 1 μg of anti-TCF4 antibody (Cell Signaling Technology, 2566) was added to the reaction solution to immunoprecipitate DNA fragments. The resulting immunoprecipitated (IP) DNA was compared with the DNA precipitated with anti-mouse IgG antibody (Abcam, ab190475) using quantitative PCR (qPCR) with SYBR Green (cat. no. 4472908) for F1, F2, or F3 regions; Thermo Fisher Scientific, Inc.), according to the manufacturer's protocol. ChIP-PCR was performed with an initial denaturation at 95°C for 3 min, followed by 40 cycles of denaturation for 30 s at 95°C, annealing for 30 s at 58°C, and extension at 72°C for 30 s, followed by a final extension at 72°C for 5 min. *GAPDH* was used as a reference gene to normalize the data. The primer sequences for qRT-PCR are listed as follow: F1 (F: ATCTTGAGGGAGACTTGGACA, R: CTCTGGATGAATACCTGTGGC), F2 (F: CTCTGAGTGAGTCGCGAGGTTAT, R: G AGTTGGTCTCCAATGTTGTTTG), and F3 (F: TGTGATT CAAGAGCTCGAGAC, R: AAGCTCGAATGACGTA CGTTC).

Total RNA extraction, cDNA synthesis, and qRT-PCR

Approximately 2 μg of total RNA from C57BL/6 mouse kidney cells was reverse-transcribed using the GoScript Reverse Transcription Kit (Reverse Transcription System, Promega) as per the manufacturer's methods. Gene expression was quantified as described previously via qRT-PCR assay (Xuan *et al*., 2016). The primers information are listed as follow: GAPDH (F: GCCAAGGTCATCCATGACAACT, R:GAGGGGCCATCCACAGTCTT), FGF1 (F: TGCTCTACTGCAGCAACG, R: C TAGTCAGAAGACACCGG), FGFR2 (F: CAAGAAC GGCGGCTTCTTC, R: GGAAGAAACAGTATGGCCT) FGR3 (F: CAAGCTCTACTGCGCTACC, R: GTCCAC CTGTATGCAGCT), FGF4 (F: TACTGCAACGTGG GCATC, R: GGAAGTGGGTTACCTTCA), FGF5 (F: GAAGTAGCGCGACGTTTTC, R: GGCTTAACACA CTGGCTTC), FGG6 (F: CTCTACTGCAACGTGGG C,R:GGAAGTGAGTGACAGTCA), FGF7 (F: AGAC TGTTCTGTCGCACC, R: CCGCTGTGTGTCCATTT AG), FGF8 (F: ACCTACCAGCTCTACAGCC, R: GG CGGGTAGTTGAGGAACT), FGF9 (F: CTGCAGGA CTGGATTTCATTT, R: GTTCAGGTACTTTGTCA GGG), FGF10 (F: TGTCCGCTGGAGAAGGCTGT TC, R:CTATGTTTGGATCGTCATGG), FGF11 (F: ATCGTCACCAAACTGTTCTG, R: CAGGAACAC TGTGGAGAGAA), FGF12 (F: TCAGCCAGCAGG GATATTTC, R: CACGACTTTGCCTCCATTCA), FGF13 (F: TAACCTCATCCCTGTGGG, R: GAGAA CTCCGTGAGATCG), FGF14 (F: CAACCTCATCC CAGTGGGA, R: GGGACTGTTTCACCAACATC), FGF15 (F: ACTCCGCTGGTCCCTATGTC, R: CTAC ATCCTCCACCATCCT), FGF16 (F: GCTTCCACC TTGAGATCTTC, R: GAGATCTCTGGACATGGAG) FGF17(F:CCAGCTCTACAGCCGGAC, R: GGGGC GGAGCCCACAAAT), FGF18 (F: CCAGCTCTATA GCAGGAC, R: GCTTGGTGACTGTGGTGT), FGF 19 (F: AACTTTATCCCCATATTTCACC, R: GAAG CTGGGACTCTTCACT), FGF20 (F: TCAGAGAA ATTGACTTCTG, R: GTGTACATCAGTAGGTCTT), FGF21 (F: GATGACGACCAAGACACTG, R: CGGC CCTGTAAAGGCTCT), FGF22 (F: GCCTCTTCTC CTCCACTC, R: CGAGACCAAGACTGGCAG). FG F23 (F: ACAGCCAGGACCAGCTATC, R: CTCGCGAGAGCAGGATACA), ANXA4 (F: ACCAGCAGCAATATGGACGG, R: TTCGGTTCCGGGAACAGAG), CTNNB1 (F: TCGCCAGGATGATCCCAGC, R: GC CCATCCATGAGGTCCTG), SMO (F: ACCTATGCC TGGCACACTTC, R: AGGAAGTAGCCTCCCACGAT, PTCH (F: CAAACTCCTGGTGCAAACCG, R: CCGGGATTCTCAGCCTTGTT), and GLI1 (F: CCAGAGTTCAAGAGCCTGG. R: CC TCGCTCCATAAGGCTCAG).

Western blot analysis

Protein was extracted from cells using a lysis solution (7 M urea, 2 M thiourea, 40 mM Trizma base, 2% CHAPS, 1% protease inhibitor, and 40 mM dithiothreitol (DTT)). The cell lysates were centrifuged at 15,000 × *g* for 15 min, and the supernatants were harvested for total protein concentration measurement via the Bradford protein assay (Bio-Rad, Richmond, CA, USA). Next, 20 μg of protein from each sample was resolved using the SDS-PAGE and subsequently transferred onto Immobilon-P Transfer Membranes (MILLIPORE JAPAN, Tokyo, Japan). The membranes were incubated in 1× TBS containing 0.05% Tween-20 and 5% milk for 2 h and incubated further with the primary antibodies at 25°C for 1 h. Anti-GAPDH (1:2500, Abcam, ab9485), anti-phospho-SAPK/JNK (Thr183/Tyr185) antibody (1:1000, Cell Signaling Technology, 4668), anti-JNK1 + JNK2 + JNK3 antibody (1:1000, Abcam, ab179461), anti-phospho-AKT (Ser473) antibody (1:2000, Cell Signaling Technology, 4060), anti-p-IκBα antibody (1:500, Santa Cruz Biotechnology, sc-8404), anti-β-catenin antibody (1:1000, Cell Signaling Technology, 8480), anti-AKT antibody (1:1000, Cell Signaling Technology, 4691), anti-β-catenin antibody (1:2000, Abcam, ab32572), and anti-ANXA4 antibody (1:2000, Abcam, ab256456) were used as primary antibodies. After incubation, the membranes were washed with 1× TBS twice and incubated for 1 h with an anti-mouse or anti-rabbit HRP-linked secondary antibody (1:2000, Cell Signaling Technology). Antigen-antibody complexes were detected with an electrochemiluminescence (ECL) kit (GE healthcare). The protein band density was quantified using the ImageJ software (National Institute of Health, Bethesda, MD, USA), and the relative levels were normalized to GAPDH levels.

Statistical analysis

Prism 5 (GraphPad Software, San Diego, CA) software was used for statistical analysis. Student's *t*-test was used to analyze significant differences between two groups.

Results

Expression patterns of FGFs in C57BL/6 mouse kidney cells

qRT-PCR was performed to evaluate the expression levels of 23 FGF family member genes in C57BL/6 mouse kidney cells. The results indicate that *FGF1*, *5*, *7*, *8*, *9*, *10*, *11*, *12*, *16*, and *17* exhibited the highest expression levels among the 23 *FGFs*. Among these, *FGF9* exhibited the highest expression, followed by *FGF1*. Meanwhile, *FGF2*, *FGF6*, *FGF13*, *FGF14*, *FGF19*, *FGF20*, *FGF21*, and *FGF23* were found to be rarely expressed in the kidney cells (Fig. 1).

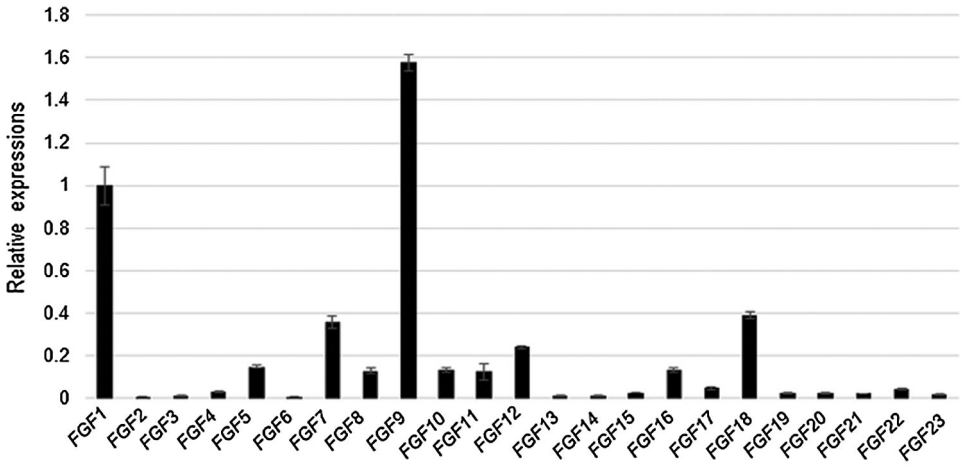

FIGURE 1. *FGF* expression patterns in kidney cells.
The expression levels of *FGFs* were analyzed in a kidney cell line by qRT-PCR and normalized against *GAPDH*. The mean ± SE indicates the error of three replicates, and the experiments were repeated at least three times.

Overexpression of FGF9 promotes kidney cell proliferation

As *FGF9* was the predominantly expressed *FGF* in kidney cells, its function was further investigated via overexpression in C57BL/6 mouse kidney cells. The qRT-PCR results indicate that the *FGF9* expression levels, but not those of *FGF1* or *FGF21*, were higher in the overexpressed cells compared to those in the non-transfected control cells (Fig. 2A). Using the *FGF9*-overexpressed cells, the proliferation rate was examined by CCK-8, and cell density measurement showed that *FGF9* overexpression significantly promoted the proliferation of C57BL/6 cells (Fig. 2B). Next, AKT and JNK levels in the control and *FGF9* overexpressing cells were analyzed. Western blotting results indicate that *FGF9* overexpression induced phosphorylation of AKT and JNK without affecting the total AKT or JNK levels (Figs. 2C and 2D).

Screening the FGF9-regulating transcriptome

To screen *FGF9*-regulating genes and pathways, RNA-seq based transcriptome analysis was performed by using the *FGF9*-overexpressing and control C57BL/6 mouse kidney cells. The RNA-seq results indicate that a total of 641 genes were differentially expressed following the overexpression of *FGF9* (1.5-fold change; $P < 0.05$). Among these, 365 downregulated genes and 276 upregulated genes were identified (Fig. 3A). Further, qRT-PCR revealed that the

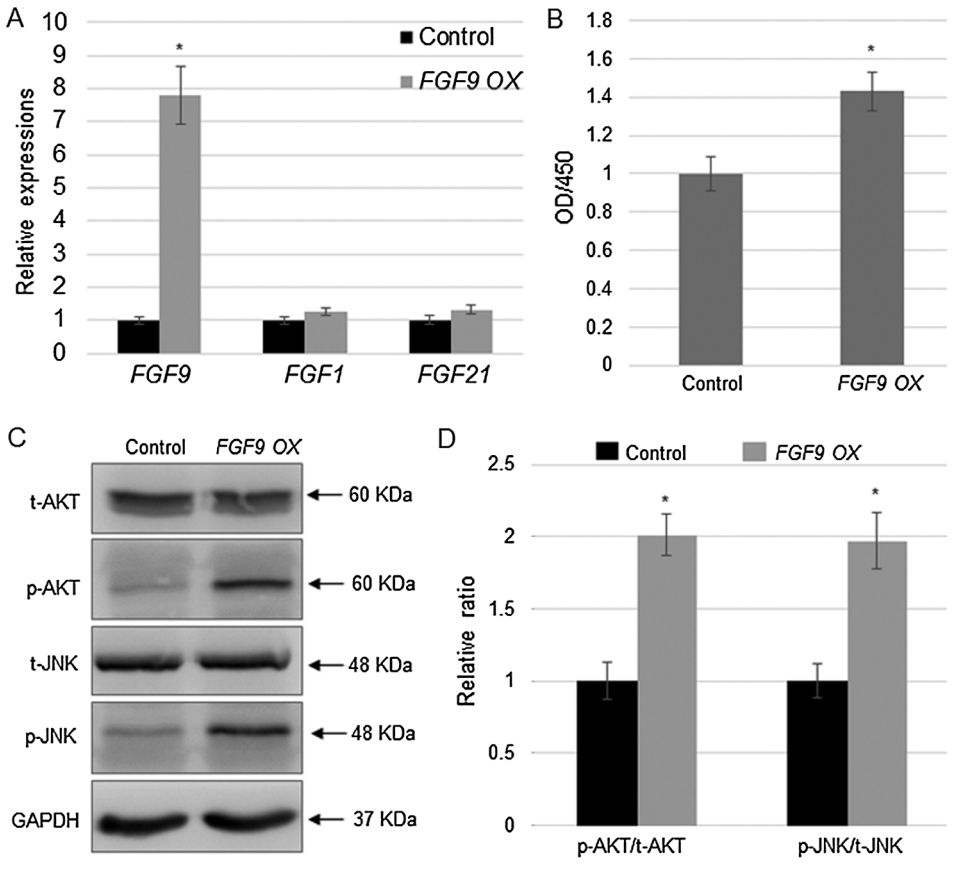

FIGURE 2. *FGF9* overexpression activates cell proliferation and induces AKT and JNK phosphorylation.
(A) qRT-PCR was used to detect *FGF9*, *FGF1*, and *FGF21* expression levels in control and *FGF9*-overexpressed C57BL/6 cells. The mean ± SE indicates the error of three replicates and the experiments were repeated at least three times. (B) Cell density was analyzed using the MTT assay after 3 days of *FGF9* overexpression. The mean ± SE indicates the error of three replicates. (C) t-AKT, p-AKT, t-JNK, and p-JNK levels were assessed by immunoblotting. GAPDH was used as an internal control. The molecular weights of each band are presented, and corresponding bands are indicated by arrowheads. (D) Calculated band density, presented in (C). Data represent the mean ± SE (N = 3). *$P < 0.05$, significant differences between control and *FGF9* overexpressed group.

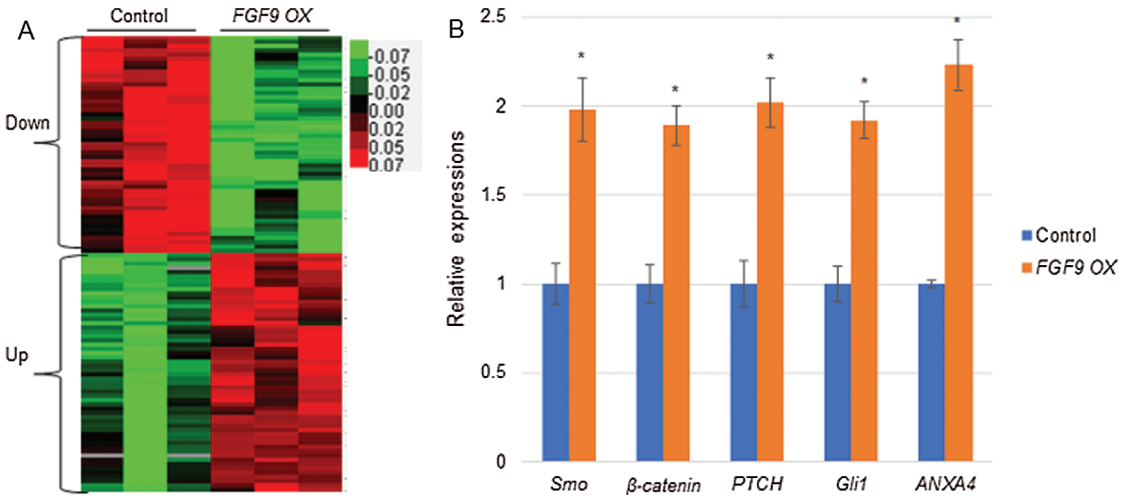

FIGURE 3. Heatmap and gene expression analysis.
(A) Heatmap represents differentially expressed genes following *FGF9* overexpression. (B) qRT-PCR was performed to analyze *SMO*, *CTNNB1*, *PTCH*, *GLI1*, and *ANXA4* expression in the control and *FGF9* overexpressed C57BL/6 cells. The mean ± SE indicates the error of three replicates. Significant differences between the control and *FGF9* overexpressed group are shown (*$P < 0.05$).

expression of WNT pathway genes (*SMO*, *CTNNB1*, and *PTCH*), hedgehog pathway genes (*GLI1*), and *ANXA4* was upregulated upon *FGF9 overexpression*, which was consistent with the RNA-seq data (Fig. 3B). The differentially expressed genes were further analyzed for their association with biological process GO terms. GO analysis indicated that 31 terms were enriched for these differentially expressed genes ($P < 0.01$) and that they were involved in diverse biological processes, including multicellular organismal development, nucleosome assembly, DNA-template transcription, and positive regulation of interleukin (IL)-10 secretion (Fig. 4A). In addition, out of the 641 differentially expressed genes, 102 were classified into known pathways ($P < 0.05$). Pathway analysis using the KEGG database was then performed to classify the differentially expressed genes. The dendrograms, a portion of which are presented in Fig. 4B, demonstrate the significance of the seven up- and nine downregulated pathways, including WNT, NF-κB, and hedgehog signaling pathways.

β-catenin knockdown inhibits kidney cell proliferation

As *FGF9* overexpression activated the expression of WNT pathway genes (*SMO*, *CTNNB1*, and *PTCH*), the expression of the key WNT signaling transcription factor, i.e., β-catenin was analyzed by western blot analysis. In agreement with the qRT-PCR results, β-catenin accumulated to a greater extent in the *FGF9*-overexpressing cells as compared to that in the control cells (Figs. 5A and 5B). Further, the role of β-catenin in kidney cell proliferation was examined using a specific shRNA against β-catenin (*CTNNB1)* and NC siRNA (control) in C57BL/6 cells (Fig. 5C). Moreover, to verify the qPCR results, Western blot analysis was performed to

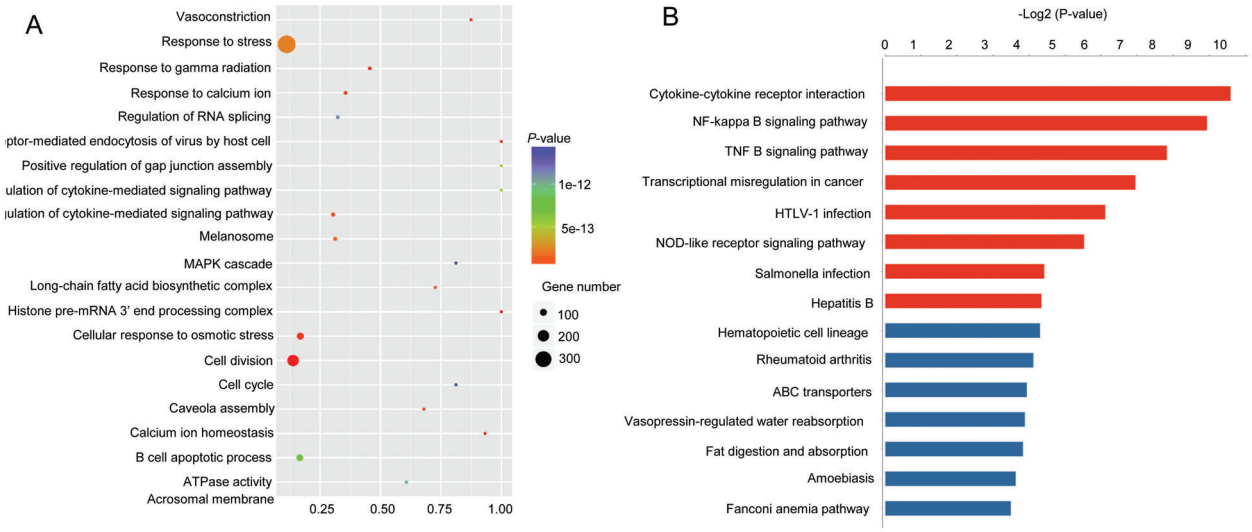

FIGURE 4. GO and KEGG analyses of FGF9-regulating genes.
The differentially expressed genes upon overexpression of *FGF9* were classified based on GO terms KEGG terms. (A) The differentially expressed genes are classified mainly into 21 GO terms, including Response to stress, MAPK cascade, and cell division. (B) The differentially expressed genes are enriched to 15 KEGG pathways, including TNF B signaling, Hepatitis B, and ABC transporters.

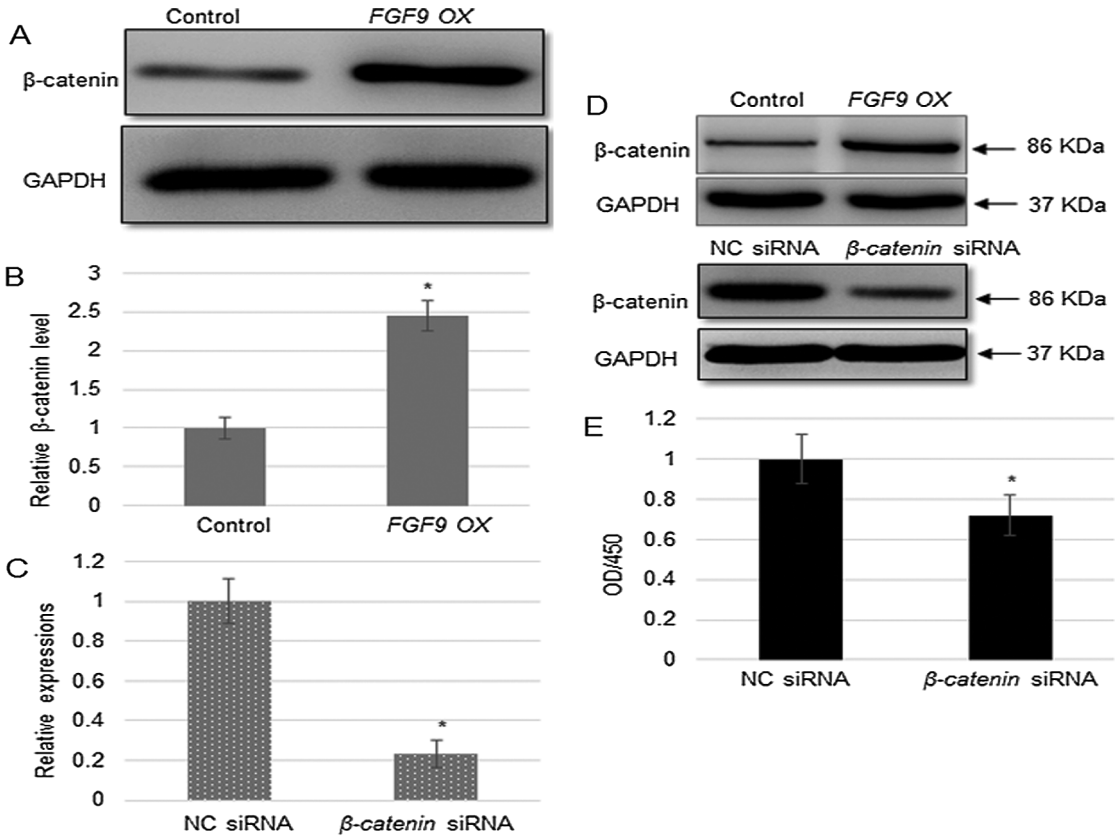

FIGURE 5. β-catenin expression and *CTNNB1*-induced suppression of cell proliferation.
(A) Detection of β-catenin and GAPDH levels in the control and *FGF9*-overexpressed C57BL/6 cells via western blotting. (B) Analysis of density for each band shown in (A). The mean ± SE indicates the error of three replicates. Significant differences between the control and *FGF9*-overexpressed C57BL/6 cells are shown (*$P < 0.05$). (C) The qRT-PCR analysis quantified *CTNNB1* expression level in the NC siRNA (control) and cells with *CTNNB1* suppression. The mean ± SE indicates the error of three replicates. Significant differences between the control and cells with *CTNNB1* suppression are shown (*$P < 0.05$). (D) β-catenin level analyzed in control and *FGF9* OX or NC siRNA and *CTNNB1* siRNA-transfected C57BL/6 cells. *GAPDH* was used as the loading control. (E) Cell proliferation rate was calculated by MTT assay in the control and cells with *CTNNB1* suppression. The mean ± SE indicates the error of three replicates. *$P < 0.05$, significant differences between the control and cells with *CTNNB1* suppression.

analyze β-catenin protein levels. The results indicate that β-catenin level was higher in *FGF9 OX* than that in the control, while it was significantly lower in *CTNNB1* siRNA than in NC siRNA transfected cells (Fig. 5D). In addition, *CTNNB1* knockdown significantly inhibited kidney cell proliferation (Fig. 5E).

ANXA4 positively regulates kidney cell proliferation downstream of CTNNB1

ANXA4 was induced by *FGF9* overexpression; therefore, its expression level was examined in *CTNNB1* knockdown cells. The qRT-PCR results show that *CTNNB1* suppression reduced *ANXA4* expression (Fig. 6A). Moreover, as ANXA4 was previously reported to play a role in the proliferation of hepatocellular carcinoma cells (Liu *et al.*, 2017), its function in kidney cell proliferation was further examined. The NC shRNA and specific shRNA were confirmed to significantly downregulate the expression of *ANXA4* at transcript (Fig. 6B) and protein levels (Fig. 6C), whereas *ANXA4* knockdown significantly inhibited kidney cell proliferation (Fig. 6D). As the β-catenin complex functions as a transcription activator to regulate downstream gene expression, the potential binding between the transcription factor complex, containing TCF4 and β-catenin, to the *ANXA4* promoter region was investigated. The TCF4 or β-catenin antibody immunoprecipitation and subsequent ChIP-PCR showed that the TCF4 and β-catenin complex bound to F2, not the F1 or F3 regions, in the *ANXA4* promoter (Fig. 6E).

Discussion

The kidney is a highly complex organ that is integral to the maintenance of salt, water, and acid-base balance, while also serving as a filter to secrete waste products from the body (Márquez *et al.*, 2002). Although the role that cell proliferation plays in general tissue maturation is well-characterized, the underlying mechanism associated with kidney cell proliferation remains largely unknown. Meanwhile, considering that studies have reported upregulation of FGF9 and FGF1 in adult rat kidney cortical and outer medullary tissues (Cancilla *et al.*, 2001), we sought to verify the expression patterns of FGFs and to characterize the function of the predominately expressed FGF in kidney cell proliferation. FGFs play a key role in diverse biological processes, including protection against diabetes-induced complications, cell migration and proliferation, and sugar metabolism, as well as skin wound

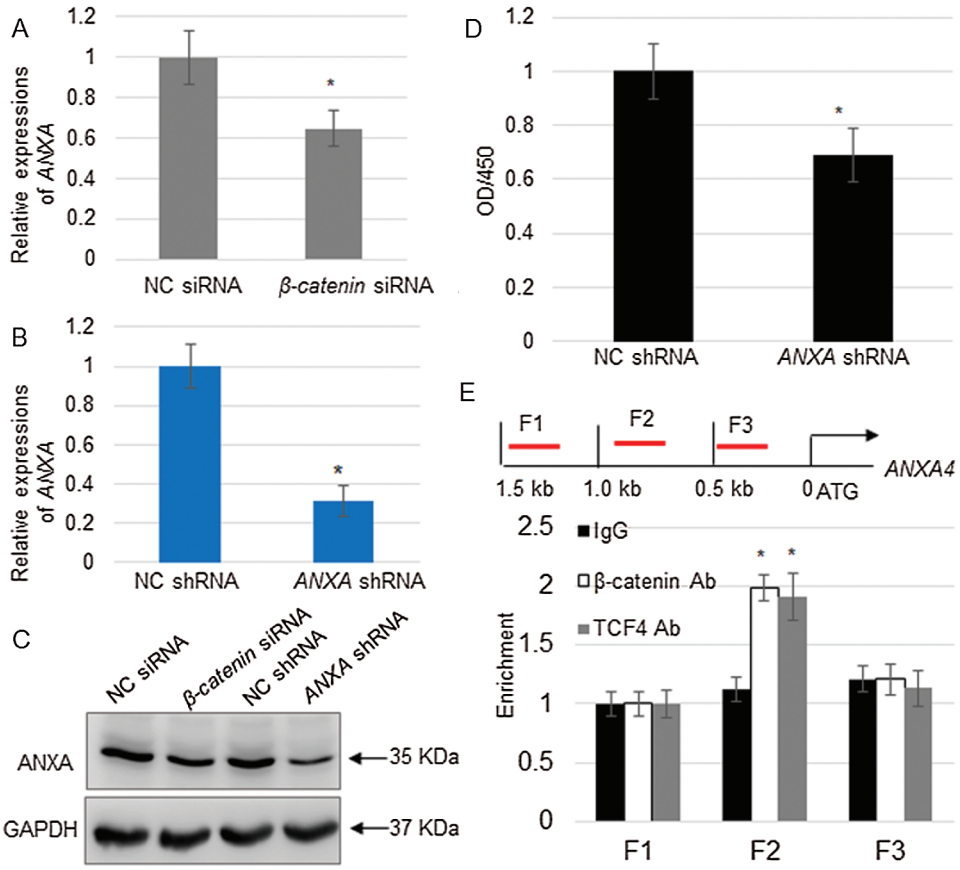

FIGURE 6. β-catenin complex directly activates *ANXA4* expression.
(A) *ANXA4* expression level analyzed in cells transfected with NC siRNA and shRNA-mediated *CTNNB1*. The mean ± SE indicates the error of three replicates. Significant differences between the NC siRNA and cells with *CTNNB1* knockdown by shRNA (*$P < 0.05$). (B) *ANXA4* expression was analyzed in NC siRNA and cells with *ANXA4* knockdown by shRNA. The mean ± SE indicates the error of three replicates. Significant differences between the control and cells with *ANXA4* suppression are shown (*$P < 0.05$). (C) ANXA4 protein abundance quantified in cells with NC siRNA and in cells with *CTNNB1* knockdown or NC shRNA and cells with *ANXA4* knockdown transformed C57BL/6 cells. *GAPDH* was used as the loading control. (D) Cell proliferation in NC shRNA and cells with *ANXA4* knockdown. The mean ± SE indicates the error of three replicates. Significant differences between the NC shRNA and cells with *ANXA4* knockdown groups are shown (*$P < 0.05$). (E) Schematic diagram indicating the PCR amplified region (F1, F2, and F3) within 1.5 kb of the *ANXA4* promoter. ChIP-PCR was performed to analyze the binding of TCF4 or β-catenin transcription factor complex to the F1, F2, and F3 regions in the *ANXA4* promoter. The mean ± SE indicates the error of three replicates. Significant differences between the IgG and β-catenin Ab or TCF4 Ab immunoprecipitation groups are shown (*$P < 0.05$). IgG, immunoglobin; Ab, antibody.

repair. Specifically, FGF9 was reported to protect against fibrosis in cardiac fibroblasts (Sun *et al.*, 2019), whereas its abnormal activation during anorectal development in rat embryos resulted in anorectal malformations (Liu *et al.*, 2019). FGF9 was also shown to alter the Wallerian degeneration process by accelerating macrophage infiltration (Lv *et al.*, 2019). Additionally, FGF9 has been identified as a potential novel biomarker for the diagnosis of prostate cancer (Cui *et al.*, 2019), suggesting that it has multiple functions in different tissues. So far, FGF23 and its partner klotho function in combination to protect against early chronic kidney disease in Type 2 diabetes. However, the function of FGF9 in kidney cells has not been analyzed.

Using C57BL/6 mouse kidney cells, 23 *FGFs* were examined for their expression patterns. The results suggest that in this cell line, *FGF1* and *FGF9* are the two predominant members based on their transcription levels, with *FGF9* exhibiting the highest expression among the 23 *FGFs*. As compared to these two *FGFs*, the other FGFs either showed low expression levels or negligible expression. However, extensive analyses have also found that *FGF21* is significantly induced by wounding, drugs, and starvation (Lin *et al.*, 2013; Liang *et al.*, 2014; Lin *et al.*, 2014; Song *et al.*, 2016a; Song *et al.*, 2016b), thereby implicating it in the protection of the liver and heart from injury, in glucose homeostasis, and skin wound healing. Hence, other *FGFs* might also become activated under certain conditions in kidney cells.

Further, *FGF9* overexpression promotes C57BL/6 cell proliferation and activates JNK and AKT similar to bFGF stimuli (Xuan *et al.*, 2016), suggesting that FGF9, and potentially other FGFs, may activate similar downstream signaling events. To further elucidate the FGF9 regulatory mechanism, RNA-seq analysis was performed using *FGF9*-overexpressing C57BL/6 mouse kidney cells. The expression of many genes was altered upon the activation of FGF9-mediated signaling, including 365 downregulated genes and 276 upregulated genes. These genes were enriched in 31 GO terms, including positive regulation of IL-10 secretion, nucleosome assembly, DNA-template transcription, and

multicellular organismal development. Additionally, KEGG analysis showed that 16 pathways were significantly enriched, including WNT, NF-κB, and hedgehog signaling pathways. These findings imply that FGF9 might regulate inflammatory responses by modulating NF-κB signaling. Hence, further studies to investigate the role of FGF9 in protecting the kidney under disease conditions will be of significant interest.

Wnt signaling is involved in cell differentiation, survival and proliferation (Gordon and Nusse, 2006), while hedgehog signaling plays important roles in the development of invertebrate and vertebrate organisms and acts as the key regulator in diverse cellular processes (Bushman, 2007). Wnt pathway genes (*SMO*, *CTNNB1*, and *PTCH*) and the hedgehog pathway gene (*GLI1*) are the key players and significantly respond to *FGF9* overexpression. Further analysis following the knockdown of *CTNNB1*, a master regulator of WNT signaling, inhibited C57BL/6 mouse kidney cell proliferation. Interestingly, *CTNNB1* suppression reduced the expression of *ANXA4*, which was induced by *FGF9* overexpression. ANXA4 was previously reported to play a role in the proliferation of hepatocellular carcinoma cells (Liu *et al*., 2017), while its suppression inhibited C57BL/6 mouse kidney cell proliferation, suggesting that β-catenin may partially regulate *ANXA4* to regulate C57BL/6 cell proliferation.

β-catenin-TCF/LEF forms a transcription factor complex that binds to the putative *cis*-elements ($^{T}/_{A}{}^{C}/_{G}$AAAG) present in the promoter region of downstream genes to regulate diverse biological processes (Schuijers *et al*., 2014). The ChIP assay using β-catenin antibody further revealed that this transcription complex binds to the *ANXA4* promoter. Additionally, TCF4, a member of the β-catenin complex that binds to DNA sequences, was also confirmed to directly bind the promoter region of *ANXA4*. This result further confirmed that β-catenin functions upstream to control *ANXA4* transcription, by which C57BL/6 cell proliferation was modulated. Our findings provide evidence that the predominant expression of FGF9 in kidney cells might be important for cell activation and proliferation and that the FGF9-β-catenin-ANXA4 pathway may be involved in this process. Therefore, this study expands the current understanding of FGF9 signaling and describes a new regulatory mechanism for understanding kidney cell proliferation.

In conclusion, this study employed the C57BL/6 mouse kidney cell line to identify the predominantly expressed *FGFs* in kidney cells. Our results found *FGF9* to be the most dominantly expressed, while *FGF9* overexpression resulted in the promotion of cell proliferation. We also demonstrated that *FGF9*-overexpressing cells accumulate more β-catenin than control cells, while *CTNNB1* or *ANXA4* knockdown inhibited cell proliferation. Hence, our results revealed that *FGF9* promotes cell proliferation via the activation of *ANXA4*, which serves to broaden our understanding of the FGF regulatory mechanism and provides scope for further exploration of FGF-regulated cell proliferation.

Conclusion

FGFs play a significant role in a broad spectrum of biological processes like cell migration and proliferation. However, their expression patterns in kidney cell proliferation remain poorly understood. In the current study, we used the C57BL/6 mouse kidney cell line to identify the dominantly expressed *FGFs* in kidney cells. Our results revealed FGF9 to be the most dominantly expressed, while *FGF9* overexpression resulted in the promotion of cell proliferation. RNA-seq based transcriptome analysis revealed differentially expressed genes in *FGF9* overexpressed cells. The results of qRT-PCR were consistent with the RNA-seq data. We also demonstrated that the *FGF9* overexpressed cells accumulated more β-catenin than the control cells, while the suppression of *β-catenin* or *ANXA4* resulted in inhibition of cell proliferation. In summary, our results showed FGF9 to be the most dominantly expressed in the kidney cells. It was shown to promote cell proliferation via activation of *ANXA4*. Our results extend the understanding of the FGF regulatory mechanism and provide scope for further exploration of FGF-regulated cell proliferation.

Acknowledgement: We appreciate very much the colleges from the School of Bioengineering, Wuhu Institute of Technology for the critical reading of our manuscript.

Author Contribution: The authors confirm contribution to the paper as follows: Study conception and design: Ting Li; data collection: Xinhui Sun; analysis and interpretation of results: Ting Li. Nannan Li; draft manuscript preparation: Ting Li. Hongmin Guo. All authors reviewed the results and approved the final version of the manuscript.

Availability of Data and Materials: The readers can access the data used in the study by contact corresponding author.

Funding Statement: This work was funded by Wuhu Institute of Technology Talent Project [wzyrc201801], the Natural Science Foundation of Anhui Province [KJ2018A0691], and the Project of Cultivating Outstanding Talents in Colleges [gxgwfx2019072] and Science and Technology Development Plan Project of TCM.

Conflicts of Interest: The authors declare that they have no conflicts of interest to report regarding the present study.

References

Bushman W (2007). Hedgehog signaling in development and cancer. In: Chung LWK, Isaacs WB, Simons JW (eds.), *Prostate Cancer Contemporary Research*. pp. 107–118. Totowa, NJ: Humana Press.

Cancilla B, Davies A, Cauchi JA, Risbridger GP, Bertram JF (2001). Fibroblast growth factor receptors and their ligands in the adult rat kidney. *Kidney International* **60**: 147–155. DOI 10.1046/j.1523-1755.2001.00781.x.

Consortium GO (2006). The gene ontology (GO) project in 2006. *Nucleic Acids Research* **34**: D322–D326. DOI 10.1093/nar/gkj021.

Cross DA, Alessi DR, Cohen P, Andjelkovich M, Hemmings BA (1995). Inhibition of glycogen synthase kinase-3 by insulin mediated by protein kinase B. *Nature* **378**: 785–789. DOI 10.1038/378785a0.

Cui G, Shao M, Gu X, Guo H, Zhang S, Lu J, Ma H (2019). The value of FGF9 as a novel biomarker in the diagnosis of prostate cancer. *Artificial Cells, Nanomedicine, and Biotechnology* **47**: 2241–2245. DOI 10.1080/21691401.2019.1620250.

Deval E, Friend V, Thirant C, Salinas M, Jodar M, Lazdunski M, Lingueglia E (2006). Regulation of sensory neuron-specific acid-sensing ion channel 3 by the adaptor protein Na^+/H^+ exchanger regulatory factor-1. *Journal of Biological Chemistry* **281**: 1796–1807. DOI 10.1074/jbc.M509669200.

Draghici S, Khatri P, Tarca AL, Amin K, Done A, Voichita C, Georgescu C, Romero R (2007). A systems biology approach for pathway level analysis. *Genome Research* **17**: 1537–1545. DOI 10.1101/gr.6202607.

Dubrulle J, Pourquié O (2004). fgf8 mRNA decay establishes a gradient that couples axial elongation to patterning in the vertebrate embryo. *Nature* **427**: 419–422. DOI 10.1038/nature02216.

Dunnick J, Brix A, Cunny H, Vallant M, Shockley K (2012). Characterization of polybrominated diphenyl ether toxicity in Wistar Han rats and use of liver microarray data for predicting disease susceptibilities. *Toxicologic Pathology* **40**: 93–106. DOI 10.1177/0192623311429973.

Dupuy D, Bertin N, Hidalgo CA, Venkatesan K, Tu D, Lee D, Rosenberg J, Svrzikapa N, Blanc A, Carnec A, Carvunis AR, Pulak R, Shingles J, Reece-Hoyes J, Hunt-Newbury R, Viveiros R, Mohler WA, Tasan M, Roth FP, Le Peuch C, Hope IA, Johnsen R, Moerman DG, Barabási AL, Baillie D, Vidal M (2007). Genome-scale analysis of *in vivo* spatiotemporal promoter activity in *Caenorhabditis elegans*. *Nature Biotechnology* **25**: 663–668. DOI 10.1038/nbt1305.

Feldman B, Poueymirou W, Papaioannou VE, DeChiara TM, Goldfarb M (1995). Requirement of FGF-4 for postimplantation mouse development. *Science* **267**: 246–249. DOI 10.1126/science.7809630.

Goldfarb M (1996). Functions of fibroblast growth factors in vertebrate development. *Cytokine & Growth Factor Reviews* **7**: 311–325. DOI 10.1016/S1359-6101(96)00039-1.

Gordon MD, Nusse R (2006). Wnt signaling: Multiple pathways, multiple receptors, and multiple transcription factors. *Journal of Biological Chemistry* **281**: 22429–22433. DOI 10.1074/jbc.R600015200.

Grigo K, Wirsing A, Lucas B, Klein-Hitpass L, Ryffel GU (2008). HNF4α orchestrates a set of 14 genes to down-regulate cell proliferation in kidney cells. *Biological Chemistry* **389**: 179–187. DOI 10.1515/BC.2008.011.

Heo J, Sachs F, Wang J, Hua SZ (2012). Shear-induced volume decrease in MDCK cells. *Cellular Physiology and Biochemistry* **30**: 395–406. DOI 10.1159/000339033.

Ji H, Wang J, Nika H, Hawke D, Keezer S, Ge Q, Fang B, Fang X, Fang D, Litchfield DW, Aldape K, Lu Z (2009). EGF-induced ERK activation promotes CK2-mediated disassociation of α-catenin from β-catenin and transactivation of β-catenin. *Molecular Cell* **36**: 547–559. DOI 10.1016/j.molcel.2009.09.034.

Kanazawa S, Fujiwara T, Matsuzaki S, Shingaki K, Taniguchi M, Miyata S, Tohyama M, Sakai Y, Yano K, Hosokawa K, Kubo T, Rappoport JZ (2010). bFGF regulates PI3-kinase-Rac1-JNK pathway and promotes fibroblast migration in wound healing. *PLoS One* **5**: e12228. DOI 10.1371/journal.pone.0012228.

Lee EJ, Park EY, Mun H, Chang E, Ko JY, Kim DY, Park JH (2015). Soluble receptor for advanced glycation end products inhibits disease progression in autosomal dominant polycystic kidney disease by down-regulating cell proliferation. *FASEB Journal* **29**: 3506–3514. DOI 10.1096/fj.15-272302.

Liang Q, Zhong L, Zhang J, Wang Y, Bornstein SR, Triggle CR, Ding H, Lam KSL, Xu A (2014). FGF21 maintains glucose homeostasis by mediating the cross talk between liver and brain during prolonged fasting. *Diabetes* **63**: 4064–4075. DOI 10.2337/db14-0541.

Lin Z, Tian H, Lam KSL, Lin S, Hoo RCL, Konishi M, Itoh N, Wang Y, Bornstein SR, Xu A, Li X (2013). Adiponectin mediates the metabolic effects of FGF21 on glucose homeostasis and insulin sensitivity in mice. *Cell Metabolism* **17**: 779–789. DOI 10.1016/j.cmet.2013.04.005.

Lin Z, Wu F, Lin S, Pan X, Jin L, Lu T, Shi L, Wang Y, Xu A, Li X (2014). Adiponectin protects against acetaminophen-induced mitochondrial dysfunction and acute liver injury by promoting autophagy in mice. *Journal of Hepatology* **61**: 825–831. DOI 10.1016/j.jhep.2014.05.033.

Liu H, Zhang H, Li M, Tian H, Tang X, Bai Y (2019). Abnormal expression of Fgf9 during the development of the anorectum in rat embryos with anorectal malformations. *Gastroenterology Research and Practice* **2019**: 1–7. DOI 10.1155/2019/1986196.

Liu YY, Ge C, Tian H, Jiang JY, Zhao FY, Li H, Chen TY, Yao M, Li JJ (2017). The transcription factor Ikaros inhibits cell proliferation by downregulating ANXA4 expression in hepatocellular carcinoma. *American Journal of Cancer Research* **7**: 1285–1297.

Lu Z, Ghosh S, Wang Z, Hunter T (2003). Downregulation of caveolin-1 function by EGF leads to the loss of E-cadherin, increased transcriptional activity of β-catenin, and enhanced tumor cell invasion. *Cancer Cell* **4**: 499–515. DOI 10.1016/S1535-6108(03)00304-0.

Lu Z, Hunter T (2004). Wnt-independent beta-catenin transactivation in tumor development. *Cell Cycle* **3**: 571–573.

Lv W, Deng B, Duan W, Li Y, Song X, Ji Y, Li Z, Liu Y, Wang X, Li C (2019). FGF9 alters the Wallerian degeneration process by inhibiting Schwann cell transformation and accelerating macrophage infiltration. *Brain Research Bulletin* **152**: 285–296. DOI 10.1016/j.brainresbull.2019.06.011.

Márquez MG, Cabrera I, Serrano DJ, Sterin-Speziale N (2002). Cell proliferation and morphometric changes in the rat kidney during postnatal development. *Anatomy and Embryology* **205**: 431–440. DOI 10.1007/s00429-002-0262-9.

Martin GR (1998). The roles of FGFs in the early development of vertebrate limbs. *Genes and Development* **12**: 1571–1586. DOI 10.1101/gad.12.11.1571.

Mohammadi M, Olsen SK, Ibrahimi OA (2005). Structural basis for fibroblast growth factor receptor activation. *Cytokine & Growth Factor Reviews* **16**: 107–137. DOI 10.1016/j.cytogfr.2005.01.008.

Muller T, Bain G, Wang X, Papkoff J (2002). Regulation of epithelial cell migration and tumor formation by beta-catenin signaling. *Experimental Cell Research* **280**: 119–133. DOI 10.1006/excr.2002.5630.

Nigam Sk AA, Brenner BM (1996). Development and maturation of the kidney. In: Brenner BM, Rector FC (eds.), *The kidney*. pp. 7298. Philadelphia: Saunders.

Ribeiro AL, Mendes F, Carias E, Rato F, Santos N, Neves PL, Silva AP (2019). FGF23-klotho axis as predictive factors of fractures in type 2 diabetics with early chronic kidney disease. *Journal of Diabetes Complications* **34**: 107476. DOI 10.1016/j.jdiacomp.2019.107476.

Schuijers J, Mokry M, Hatzis P, Cuppen E, Clevers H (2014). Wnt-induced transcriptional activation is exclusively mediated by TCF/LEF. *EMBO Journal* **33**: 146–156. DOI 10.1002/embj.201385358.

Song R, Yosypiv IV (2012). Development of the kidney medulla. *Organogenesis* **8**: 10–17. DOI 10.4161/org.19308.

Song Y, Ding J, Jin R, Jung J, Li S, Yang JQ, Wang AN, Li ZJ (2016a). Expression and purification of FGF21 in *Pichia pastoris* and its effect on fibroblast-cell migration. *Molecular Medicine Reports* **13**: 3619–3626. DOI 10.3892/mmr.2016.4942.

Song YH, Zhu YT, Ding J, Zhou FY, Xue JX, Jung JH, Li ZJ, Gao WY (2016b). Distribution of fibroblast growth factors and their roles in skin fibroblast cell migration. *Molecular Medicine Reports* **14**: 3336–3342. DOI 10.3892/mmr.2016.5646.

Suh JM, Jonker JW, Ahmadian M, Goetz R, Lackey D, Osborn O, Huang Z, Liu W, Yoshihara E, van Dijk TH, Havinga R, Fan W, Yin YQ, Yu RT, Liddle C, Atkins AR, Olefsky JM, Mohammadi M, Downes M, Evans RM (2014). Endocrinization of FGF1 produces a neomorphic and potent insulin sensitizer. *Nature* **513**: 436–439. DOI 10.1038/nature13540.

Sun J, Wang Z, Shi H, Gu L, Wang S, Wang H, Li Y, Wei T, Wang Q, Wang L (2019). LncRNA FAF inhibits fibrosis induced by angiotensinogen II via the TGFbeta1-P-Smad2/3 signalling by targeting FGF9 in cardiac fibroblasts. *Biochemical and Biophysical Research Communications* **521**: 814–820. DOI 10.1016/j.bbrc.2019.10.175.

Sun X, Meyers EN, Lewandoski M, Martin GR (1999). Targeted disruption of Fgf8 causes failure of cell migration in the gastrulating mouse embryo. *Genes and Development* **13**: 1834–1846. DOI 10.1101/gad.13.14.1834.

Wang X, Zhu Y, Sun C, Wang T, Shen Y, Cai W, Sun J, Chi L, Wang H, Song N, Niu C, Shen J, Cong W, Zhu Z, Xuan Y, Li X, Jin L (2017). Feedback activation of basic fibroblast growth factor signaling via the Wnt/β-catenin pathway in skin fibroblasts. *Frontiers in Pharmacology* **8**: 32.

Weston CR, Davis RJ (2001). Signaling specificity—A complex affair. *Science* **292**: 2439–2440. DOI 10.1126/science.1063279.

Xuan Y, Chi L, Tian H, Cai W, Sun C, Wang T, Zhou X, Shao M, Zhu Y, Niu C, Sun Y, Cong W, Zhu Z, Li Z, Wang Y, Jin L (2016). The activation of the NF-κB-JNK pathway is independent of the PI3K-Rac1-JNK pathway involved in the bFGF-regulated human fibroblast cell migration. *Journal of Dermatological Science* **82**: 28–37. DOI 10.1016/j.jdermsci.2016.01.003.

Yang CM, Ji S, Li Y, Fu LY, Jiang T, Meng FD (2017). β-Catenin promotes cell proliferation, migration, and invasion but induces apoptosis in renal cell carcinoma. *OncoTargets and Therapy* **10**: 711–724. DOI 10.2147/OTT.S117933.